



Stress analysis of two-dimensional perforated plates using boundary element alternating method

Chen K.T., Yang W.S.

National Chung-Hsing University, Taiwan

ABSTRACT: In this paper, the boundary element alternating method (BEAM) is developed to solve the stress concentration of two-dimensional perforated plate. This method involves the iterative superposition between the boundary element solution of a bounded plate without holes and the analytical solution of an infinite two-dimensional plate with a circular hole subjected to arbitrary normal and shear loading until the required boundary conditions of the original problem are satisfied. Excellent agreement between the solutions of the present simplified procedure and the conventional finite element techniques are observed and show the advantages of the alternating method.

1. INTRODUCTION

The determination of stress concentration is very important in solving well-known localized geometrical discontinuities in realistic engineering problems such as holes, notches, etc. Several analytical methods were developed to evaluate the stress concentrations for multiple circular holes in infinite plate [1,2]. For finite perforated plates, the finite element method (FEM) and boundary element method (BEM) were widely used to study the interaction among holes [3-5]. Numerical experiments indicate the accuracy of the stress distribution around holes obtained largely depends on the mesh size taken. It always consumes more computer time. Recent research revealed the potential of the finite element alternating method to solve the fracture problems [6,7]. The boundary element method was also used in the alternating method instead of finite element method [8]. Thus the extension of the previous works to analyze the interactions among the arbitrary distribution of multiple circular holes with various sizes is the main objective of this work.

The alternating method developed and employed herein is based on an earlier method known as the Schwartz-Neumann alternating method [9]. In the process of the alternating method, an analytical solution of the single circular hole in the infinite domain subjected to the arbitrary surface tractions over the circumference of the hole is necessary. The normal and shear loading can be expressed as Fourier series expansions. Corresponding to each harmonic functions $\sin(n\theta)$ and $\cos(n\theta)$, the solutions of stress are derived herein. These analytical solutions are then used as the fundamental solutions in the alternating method. The reversed residual stresses at the location of fictitious circular holes are repeatedly evaluated and treated as new applied loading for the next iteration until the desired accuracy is reached.

Several problems of multiple holes with different size and arrangement are analyzed for verifying the validity of this present work. The interactions among holes are studied in detail. The results are put into comparison with the conventional finite element solutions is shown to obtain the accurate stress concentration factor (SCF) with simple technique and minimal computing effort.

2. ANALYTICAL SOLUTION FOR AN INFINITE PLATE WITH A HOLE

An infinite domain with a circular hole of radius R which the center locates at $X = 0$ and $Y = 0$ is shown in Fig.1. The hole surface is subjected to arbitrary normal force $T_r(\theta)$ and shear force $T_\theta(\theta)$. Both radial and tangential loadings on the hole surface can be presented by Fourier series as:

$$T_r(\theta) = \sum_{m=0}^n a_m \cos(m\theta) + \sum_{m=1}^n b_m \sin(m\theta), \quad T_\theta(\theta) = \sum_{m=0}^n c_m \cos(m\theta) + \sum_{m=1}^n d_m \sin(m\theta)$$

Using the boundary conditions: the stresses must be zero as r tend to infinity, and the compatibility conditions of the displacement components, the stress components of the plane stress problem can then be derived as follows.

$$\begin{aligned} \sigma_r &= -a_0 \left(\frac{R}{r}\right)^2 - \left[A \left(\frac{R}{r}\right)^3 - (A-1) \left(\frac{R}{r}\right)\right] \left[a_1 \cos \theta + b_1 \sin \theta \right] + \left[B \left(\frac{R}{r}\right)^3 + (A-1) \left(\frac{R}{r}\right) \right] \left[c_1 \sin \theta - d_1 \cos \theta \right] \\ &+ \sum_{m=2}^n \left[\frac{m}{2} \left(\frac{R}{r}\right)^{m+2} - \frac{m+2}{2} \left(\frac{R}{r}\right)^m \right] \left[a_m \cos(m\theta) + b_m \sin(m\theta) \right] \\ &+ \sum_{m=2}^n \left[\frac{m+2}{2} \left(\frac{R}{r}\right)^{m+2} - \frac{m-2}{2} \left(\frac{R}{r}\right)^m \right] \left[c_m \sin(m\theta) - d_m \cos(m\theta) \right] \\ \sigma_\theta &= a_0 \left(\frac{R}{r}\right)^2 + A \left[\left(\frac{R}{r}\right)^3 + \left(\frac{R}{r}\right) \right] \left[a_1 \cos \theta + b_1 \sin \theta \right] + \left[-B \left(\frac{R}{r}\right)^3 + A \left(\frac{R}{r}\right) \right] \left[c_1 \sin \theta - d_1 \cos \theta \right] \\ &+ \sum_{m=2}^n \left[-\frac{m}{2} \left(\frac{R}{r}\right)^{m+2} + \frac{m-2}{2} \left(\frac{R}{r}\right)^m \right] \left[a_m \cos(m\theta) + b_m \sin(m\theta) \right] \\ &+ \sum_{m=2}^n \left[-\frac{m+2}{2} \left(\frac{R}{r}\right)^{m+2} + \frac{m-2}{2} \left(\frac{R}{r}\right)^m \right] \left[c_m \sin(m\theta) - d_m \cos(m\theta) \right] \\ \tau_{r\theta} &= -c_0 \left(\frac{R}{r}\right)^2 + A \left[-\left(\frac{R}{r}\right)^3 + \left(\frac{R}{r}\right) \right] \left[a_1 \sin \theta - b_1 \cos \theta \right] + \left[-B \left(\frac{R}{r}\right)^3 - A \left(\frac{R}{r}\right) \right] \left[c_1 \cos \theta + d_1 \sin \theta \right] \\ &+ \sum_{m=2}^n \left[\frac{m}{2} \left(\frac{R}{r}\right)^{m+2} - \frac{m}{2} \left(\frac{R}{r}\right)^m \right] \left[a_m \sin(m\theta) - b_m \cos(m\theta) \right] \\ &+ \sum_{m=2}^n \left[-\frac{m+2}{2} \left(\frac{R}{r}\right)^{m+2} + \frac{m}{2} \left(\frac{R}{r}\right)^m \right] \left[c_m \cos(m\theta) + d_m \sin(m\theta) \right] \end{aligned}$$

where $A = 1-\nu/4$, $B = 3+\nu/4$ and ν is the Poisson's ratio.

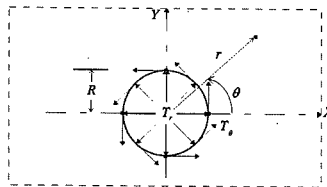


Figure 1. Arbitrary normal and shear load applied to the hole boundary in infinite domain.

3. BOUNDARY ELEMENT ALTERNATING METHOD

3.1 Alternating Procedures for An Infinite Domain Problem

Consider a two-dimensional infinitely extended solid containing k circular holes, under arbitrary hole boundary tractions, as shown in Fig. 2(a). This problem can be solved by the iterative technique in conjunction with analytical solutions. Iterative processes of the alternating method can be illustrated in Fig. 2(b)-(f), and is explained below

(1) Represent the arbitrary load distributions T_j^i on the boundary surface of the circular hole j ($j=1,2,\dots,k$) for the iterative cycle i by Fourier series, as shown in Fig. 2(a). T_j^i can be written in matrix form as.

$$\{T\}_j^i = \begin{Bmatrix} T_r \\ T_\theta \end{Bmatrix}_j^i = [A]_j^i \cdot \{P\}$$

and

$$[A] = \begin{bmatrix} a_0 & a_1 & a_2 & \dots & a_n & b_1 & b_2 & \dots & b_n \\ c_0 & c_1 & c_2 & \dots & c_n & d_1 & d_2 & \dots & d_n \end{bmatrix}$$

$$\{P\} = \{1 \quad \cos\theta \quad \cos 2\theta \quad \dots \quad \cos n\theta \quad \sin\theta \quad \sin 2\theta \quad \dots \quad \sin n\theta\}^T$$

where $[A]_j^i$ is the matrix of the hole j which is composed of the coefficients of Fourier series for the i th iteration. The superscript T designated the transpose of the matrix.

(2) Using the analytical solution obtained in the previous section, the interactive residual tractions t_{1n}^i induced by hole 1 at a fictitious hole n ($n = 2,3,\dots,k$) are computed (see Fig. 2(b)). Thus the original loading force T_2^i of the hole 2 (shown in Fig. 2(c)) must minus the interactive residual tractions t_{12}^i which is the influence of the hole 2 induced by hole 1, i.e., $T_2^i - t_{12}^i$. And the residual tractions of the other holes corresponding this residual tractions are t_{2n}^i ($n = 1,3,4,\dots,k$). In general, the residual tractions for hole k is $T_k^i - t_{1k}^i - t_{2k}^i - \dots - t_{(k-1)k}^i$, and the corresponding coefficient matrix is

$$[A]_k^i - [A]_{1k}^i - [A]_{2k}^i - \dots - [A]_{(k-1)k}^i$$

The superposition procedure can now be repeated with the next residual loads T_j^{i+1} for the iterative cycle $i+1$, as shown in Fig. 2(f). The residual loads and the corresponding coefficient matrix will be reduced after each cycle of the iteration and may be expressed as:

$$T_j^{i+1} = - \sum_{n=j+1}^k t_{nj}^i, \quad [A]_j^{i+1} = - \sum_{n=j+1}^k [A]_{nj}^i \quad j = 1,2,\dots,k-1$$

(3) Once the ratio of residual stresses to be released/permisible stress for each hole is smaller than a small value γ , say

$$\sum_{j=1}^k |T_j^{i+1}| / S < \gamma, \quad \gamma = 0.005,$$

the iteration is finished and goes to step 5. Here S is the initial stresses applied on hole surfaces. If the tractions are not negligible, the iteration is not completed and goes to step 4.

(4) Consider the residual tractions of step 2 as new applied loading acting on each hole

surface. Repeat all the iteration procedure (i.e., step 1 to step 3) until the residual tractions on each hole are negligible.

(5) Evaluate the final stress components and stress concentration factor.

3.2 Alternating Procedures for A Finite Domain Problem

Consider a two-dimensional finite plate with k circular holes subjected to arbitrary loadings, as shown in Fig. 3(a). The present BEAM can be illustrated in Fig. 3, and is explained below.

(1) Input the geometry and boundary conditions of the perforated plate, as shown in Fig.3(a).

(2) Analyze the same configuration and loading as the given problem, but without the hole using the BEM (as shown in Fig. 3(b)). We obtain the initial residual stresses σ_B^1 at the location of the original hole, and transform these stresses into the residual tractions T_j . Since the hole surfaces are traction free, reverse the sign of the residual tractions and consider the current problem as shown in Fig. 3(c).

(3) Calculate the effect between multiple holes. In Fig. 3(c), this problem may be separated into two sub-problems (as shown in Fig. 3(d)-(e)). Fig. 3(d) shows the two-dimensional infinite domain problem; an infinitely extended solid containing k circular holes, under the residual tractions $-T_j (j=1,2,\dots,k)$ on the hole surfaces. Using the alternating procedures given in the Sec. 3.1, the iterative stresses $\sigma_E^l (l=1,2,\dots)$ at everywhere for the current cycle l can be calculated. Therefore, the residual tractions $P_m^l (m=1,\dots,4)$ at the ends of the plate are obtained.

(4) Calculate the resultant stress field (i.e. $\sigma^l = \sigma_B^l + \sigma_E^l$), the final stress field (i.e. $\sigma = \sigma + \sigma^l$) and the stress concentration factors for the current iteration cycle $l (l=1,2,\dots)$.

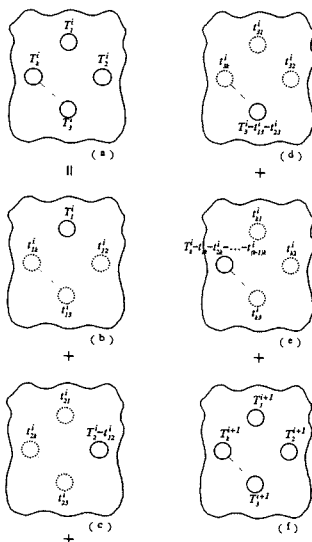


Figure 2. Alternating procedures for an infinite domain problem.

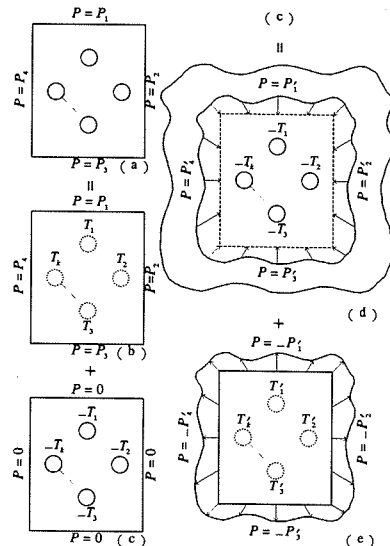


Figure 3. Alternating procedures for a finite domain problem.

(5) Once the ratios of the absolute value of the stress concentration factor increment from the current iteration l for each hole are all smaller than a small value γ , say,

$$|K^l - K^{l-1}|/K^l < \gamma, \gamma = 0.005$$

the iteration is finished and go to step 7. If the variation of stress concentration factors for each holes are not negligible, the iteration is not completed and goes to step 6.

(6) To satisfy the traction-free boundary condition of the plate (Fig. 3(c)), the residual tractions need to be reverse and considered as the applied tractions for the problem of the Fig. 3(e). Use the BEM to compute the stresses σ_B^{l+1} and transform into the residual tractions $T_j'(j=1,2,\dots,k)$ on the fictitious hole surfaces of the Fig. 3(e). Also, since the hole surfaces are traction free, reverse the sign of the residual tractions and consider the current problem similar to the Fig. 3(c). Repeat the iteration procedures (3)-(5) until the variation of stress concentration factors for each holes are negligible.

(7) Obtain the final stress field and the stress concentration factors.

4. RESULTS AND DISCUSSION

In the present article, we devote our attention to consider the effect of size of defense hole upon the SCF at the main and defense holes. A few special cases are selected based on Meguid's finite element analysis [3]. As shown in Fig. 4, a finite plate containing two equal main holes (radius D) under tension $S(N/mm^2)$ is the basic main hole system for all problems. The numerical values used in the basic modal are as follows: $D = 5 \text{ mm}$, $W = 4D$, $H = 12.5D$ and the center distance $P = 20D/3$. In this system, the maximum SCF is obtained with the value of 3.145. Based on this basic main hole system, several defense holes are introduced between the main holes, and consider as the following three conditions (as shown in Fig. 5): (I) a defense hole system, (II) two defense holes system and (III) two defense and a intermediate holes system.

Condition (I): A defense hole (radius d) is introduced between the main holes (see Fig. 5(a)). Three defense hole radii $d = D/3, 2D/3$ and $2.75D/3$ are considered. The variation of SCF along X -axis for the three defense hole radii are given in Fig. 6 and 7 about the main and defense holes, respectively. In Fig. 6, the SCF at the main hole reduces from 3.118 to 2.916 with the increased defense hole radius. In all cases considered, the value of SCF abruptly decreases near the main hole and then approaches unity at the end of the plate ($X/D = 4$). In Fig. 7, the SCF at the defense hole increases from 1.890 to 2.446 as the defense hole radius increases. To compare the results of the SCF at and near the defense hole, an entirely different trend than those of the main hole have observed.

Condition (II): Two equal defense holes (radius d) are introduced between the main holes, and the center distance between the defense holes is kept constant ($P_1 = 2D$), as shown in Fig. 5(b). Three defense hole radii are also considered as the previous condition. Fig. 8 and 9 show the variation of SCF along X -axis about the main and defense holes, respectively. For increased the defense hole radius, the SCF of the main hole reduces from 3.102 to 2.801 and the SCF of the defense hole increases from 1.578 to 2.202. The same characteristics for the main and defense holes are also observed as condition (I).

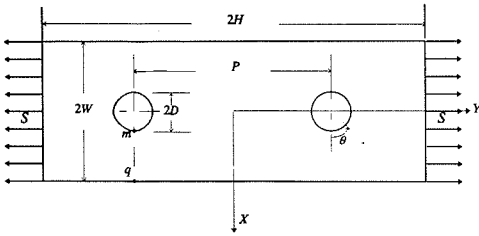
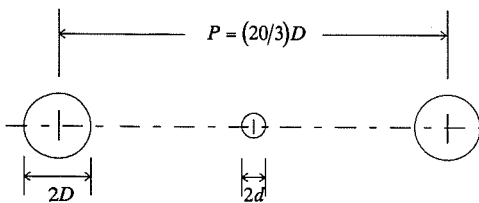
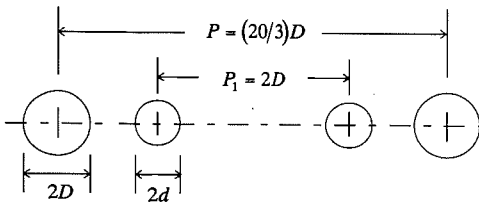


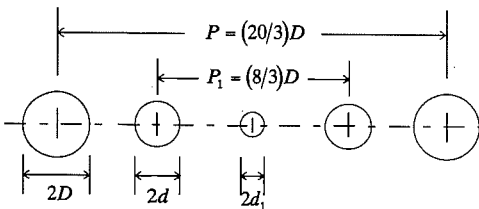
Figure 4. Basic main hole system.



a) Condition (I): a defense hole system.



b) Condition (II): two defense holes system.



c) Condition (III): two defense and a intermediate holes system.

Figure 5. The main and defense holes system.

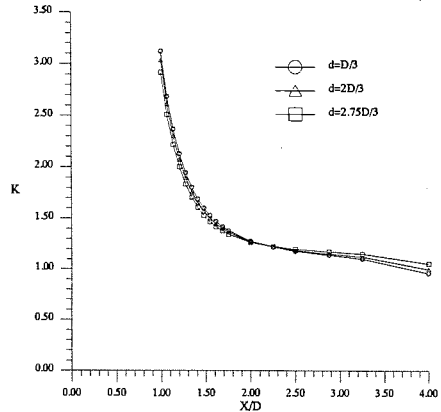


Figure 6. SCF about X-axis along the main hole for condition (I)

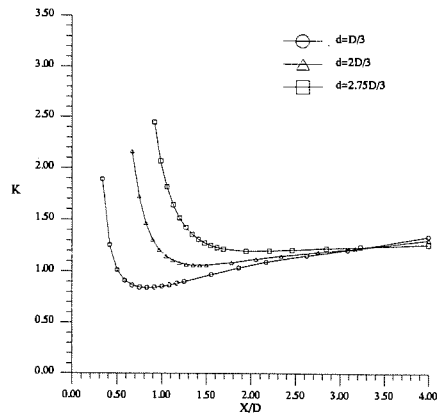


Figure 7. SCF about X-axis along the defense hole for condition (I)

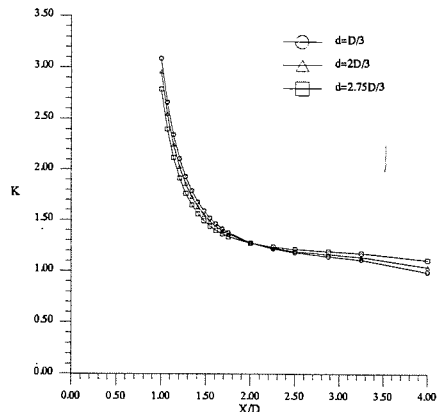


Figure 8. SCF about X-axis along the main hole for condition (II)

Table 1. The stress concentration factors for a finite plate with multiple holes

	Defense hole radius (d)	BEAM			ANSYS			REF. [3]		
		SCF			SCF			SCF		
		main hole	defense hole	intermediate hole	main hole	defense hole	intermediate hole	main hole	defense hole	intermediate hole
Main hole system		3.14			3.13			3.34		
Condition (I)	(1/3)	3.11	1.89		3.11	1.72		3.31	1.86	
	(2/3)	3.03	2.16		3.03	1.94		3.13	2.11	
	(2.75/3)	2.91	2.44		2.91	2.31		3.09	2.49	
Condition (II)	(1/3)	3.10	1.57		3.09	1.57		3.29	1.54	
	(2/3)	2.97	1.88		2.96	1.87		3.14	1.91	
	(2.75/3)	2.80	2.20		2.82	2.22				
Condition (III) $d_1 = D/4$	(1/4)	3.11	1.22	1.69	3.01	1.21	1.54	3.24	1.25	1.68
	(1/3)	3.10	1.33	1.56	3.09	1.33	1.42	3.20	1.29	1.57
	(2/3)	2.98	1.86	0.61	2.97	1.84	0.54	3.04	1.78	0.62
	(2.75/3)	2.79	2.24	-0.00	2.79	2.23	0.00	2.98	2.35	0.

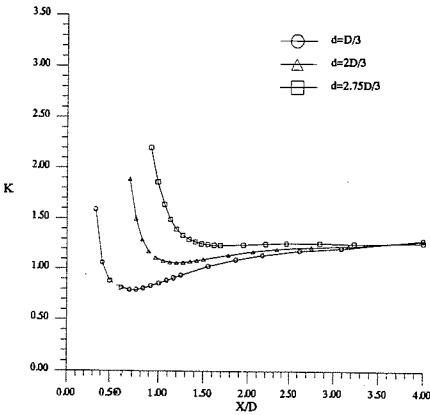


Figure 9. SCF about X-axis along the defense hole for condition (II)

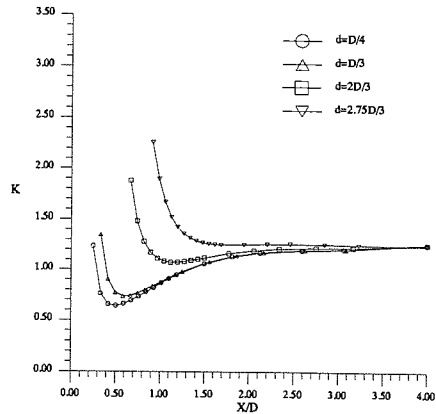


Figure 11. SCF about X-axis along the defense hole for condition (III)

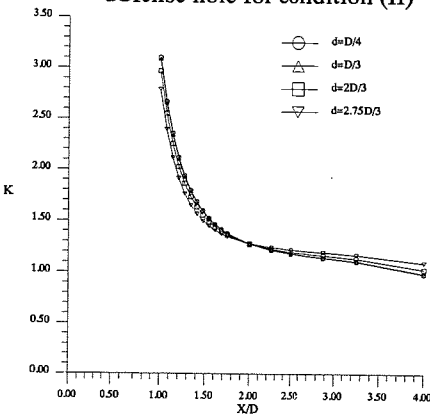


Figure 10. SCF about X-axis along the main hole for condition (III)

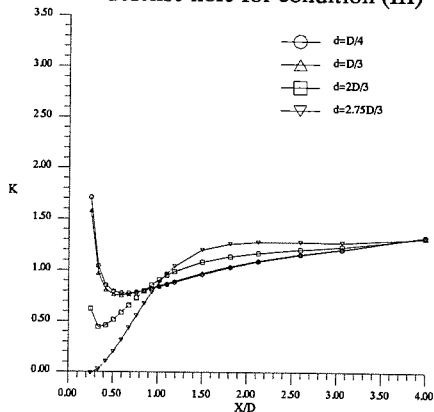


Figure 12. SCF about X-axis along the intermediate hole for condition (III)

Condition (III): A intermediate hole (radius $d_1 = D/4$) is introduced between the defense holes, and the center distance between the defense holes is taken as $P_1 = 8D/3$, as shown in Fig. 5(c). Four defense hole radii $d = D/4$, $d = D/3$, $2D/3$ and $2.75D/3$ are considered. The variation of SCF along the X -axis for all cases are given in Fig. 10–12 for the main, defense and intermediate holes, respectively. It is interesting to note that the SCF at the intermediate hole approximates to zero for the case of $d = 2.75D/3$.

All the cases are also performed by the well-known finite element package ANSYS. Table 1 shows the summary of computed SCF for all cases. The results obtained by ANSYS and Meguid [3] are also compared.

5. CONCLUSIONS

The BEAM is presented and applied to analyze the perforated plates with single or multiple holes. The interaction effects among holes and the boundary effects of finite plate can be accurately evaluated through very limited iterations and using only a very limited number of elements. The computer cost of the present computation is much less than the traditional BEM and FEM. Finally, this work can be further extended to analyze perforated plate under thermal effect, and will be presented in the near future.

REFERENCES

1. Horii, H. and S. Nemat-Nasser 1985. Elastic Fields of Interacting Inhomogeneities. *Int. J. Solids Structures* 21: 731-745.
2. Meguid, S. A. and C. L. Shen 1992. On the Elastic Fields of Interacting Defense and Main Hole Systems. *Int. J. Mech. Sci.* 34: 17-29.
3. Meguid, S. A. 1986. Finite element analysis of defense hole systems for the reduction of stress concentration in a uniaxially-loaded plate with two coaxial holes. *Engng Fract. Mech.* 25(4): 403-413.
4. Meguid, S. A. and S. X. Gong 1993. Stress Concentration Around Interacting Circular Holes: A Comparison Between Theory and Experiments. *Engng Fract. Mech.* 44: 247-256.
5. Meguid, S. A., A. L. Kalamkarov and J. Yao 1996. Analytical, numerical, and experimental studies of effective elastic properties of periodically perforated materials. *J. Engng Mater. and Tech.* 118: 43-48.
6. Chen, W. H. and C. S. Chang 1990. Analysis of multiple cracks in an infinite plate under arbitrary crack surface tractions. *Ingenieur-Archiv* 60: 202-212.
7. Ting, K., K. K. Chang and M. F. Yang 1994. Alternating method applied to analyze Mode-III fracture problems with multiple cracks in an infinite domain. *Nucl. Engng and Design* 152: 135-145.
8. Ting, K., K. K. Chang and M. F. Yang 1995. Analysis of mode-III fracture problem with multiple cracks by boundary element alternating method. *Int. J. Pressure Vessels and Piping* 62(3): 259-267.
9. Kantorovich, L. V. and V. I. Krylov 1964. *Approximate methods of higher analysis*. Interscience: New York.